Applied Water Science (2018) 8:51
https://doi.org/10.1007/s13201-018-0690-1

ORIGINAL ARTICLE

Identifying potential effects of climate change on the development of water resources in Pinios River Basin, Central Greece

G. Arampatzis[1] · A. Panagopoulos[1] · V. Pisinaras[1] · E. Tziritis[1] · F. Wendland[2]

Received: 31 March 2016 / Accepted: 11 March 2018 / Published online: 16 March 2018

Abstract

The aim of the present study is to assess the future spatial and temporal distribution of precipitation and temperature, and relate the corresponding change to water resources' quantitative status in Pinios River Basin (PRB), Thessaly, Greece. For this purpose, data from four Regional Climate Models (RCMs) for the periods 2021–2100 driven by several General Circulation Models (GCMs) were collected and bias-correction was performed based on linear scaling method. The bias-correction was made based on monthly precipitation and temperature data collected for the period 1981–2000 from 57 meteorological stations in total. The results indicate a general trend according to which precipitation is decreasing whilst temperature is increasing to an extent that varies depending on each particular RCM–GCM output. On the average, annual precipitation change for the period 2021–2100 was about − 80 mm, ranging between − 149 and + 35 mm, while the corresponding change for temperature was 2.81 °C, ranging between 1.48 and 3.72 °C. The investigation of potential impacts to the water resources demonstrates that water availability is expected to be significantly decreased in the already water-stressed PRB. The water stresses identified are related to the potential decreasing trend in groundwater recharge and the increasing trend in irrigation demand, which constitutes the major water consumer in PRB.

Keywords Climate change · Water resource regional climate models · Precipitation · Temperature · Pinios River Basin

Introduction

Mediterranean has been identified as the most vulnerable European region in terms of climate change impacts (Schröter et al. 2005; Navarra and Tubiana 2013). According to Giorgi (2006), Mediterranean region constitutes the planet's hot spot in terms of climate change effects. This is justified by the significant temperature increase and precipitation decrease with fewer wet days and drier summers as presented in several studies. More specifically, Dubrovsky et al. (2014) investigated the future trends of precipitation and temperature variation based on the results of 16 GCM runs. Their results indicate significant increase in temperature for the period 2070–2099 compared to the period 1961–1990, which is higher during summer and lower during winter and spring. In terms of precipitation, significant decrease of up to 30% was indicated on an annual basis for the south Mediterranean area, which was presented to be even higher in its westernmost and easternmost parts. Similar trends are presented by Giorgi and Lionello (2008). Jacobeit et al. (2014) reviewed a wide number of studies which investigated projected climate change trends in Mediterranean region by applying statistical downscaling techniques in model's climate data. In terms of temperature, seasonal variation in future projections indicates the best agreement. With regard to precipitation, a decreasing trend can be considered for autumn, spring and summer values for the whole Mediterranean region, while winter precipitation indicates significant variability and cannot be characterized as increasing or decreasing in general. Concerning Greece, the results of the analysis performed in precipitation and temperature data of 22 RCMs by Tolika et al. (2012) indicated an increasing trend in future temperature variation by all models, while in terms of precipitation, most of the models, but not all, presented decrement in future precipitation amount and wet day occurrence. Precipitation is also presented to be decreased by Chenoweth et al. (2011), according to which a decrement

✉ G. Arampatzis
arampgeo@gmail.com

[1] Soil and Water Resources Institute, Hellenic Agricultural Organization-Demeter, 57400 Sindos, Greece

[2] Forschungzentrum Juelich GmbH, Agrosphere Institute (IBG-3), 52425 Juelich, Germany

by 18 and 22% is indicated for precipitation in Greece by the midcentury and the end of century, respectively. Moreover, extreme precipitation events such as frequency and magnitude are expected to be increased in Greece, especially during winter (Tolika et al. 2008).

The above-described changes in precipitation and temperature variation patterns during the twenty-first century are expected to significantly affect water resource availability in Mediterranean region, while there are studies which are indicating that water yields in Mediterranean region have already been decreased, as a consequence of climate change (García-Ruiz et al. 2011; Ludwig et al. 2011). According to European Environment Agency (2009), several studies have been conducted which aim to assess the potential effects of climate change in water resources in Mediterranean region and their common conclusion is that water resource availability is expected to decrease. Milano et al. (2013) investigated the effects of climate change in water resources in Mediterranean region and their results indicated that by 2050 a significant decrease in freshwater availability is expected which ranges between 30 and 50%. Local studies of climate change impacts in water resources are also indicating significant stresses for water resources in Greece. More specifically, Pisinaras (2016) investigated potential climate change effects in an aquifer located in northeastern Greece and the results indicated a significant decrease in groundwater level, as a result of decreased groundwater recharge and increased groundwater abstractions for irrigation. A significant reduction in future water resource availability was also presented by Koutroulis et al. (2016) for Crete island (south Greece), while significant decrease in surface runoff was suggested for the next 50 years by Kalogeropoulos and Chalkias (2013) for a catchment located in Andros island.

Several hydrological modelling studies have already been performed in Pinios River Basin to assess the impacts of climate change on water resources, e.g. Mimikou and Baltas (2013), Varanou et al. (2002), indicating decreasing runoff levels and a need to adapt regional water resources management to climate change. Panagopoulos et al. (2016) applied the grid-based empirical model GROWA to assess the climate change impact for the forecasting period 2020–2080. Despite the fact that the implemented code provides a spatially distributed but temporally averaged result, the forecasted impact of climate change was pronounced as the availability of renewable water resources, i.e. the mean total runoff, was forecasted to decrease by 22–62%, depending on the examined climate change scenario.

Taking into account all the above, as well as the necessity to develop climate change impact assessment studies on the local scale, to construct sustainable development plans (Milano et al. 2013), careful evaluation of climate change data sets seems to be indispensable to comprehend climate change impact on water resources availability and spatio-temporal distribution. Against this background, the aims of this study are:

- To assess the temporal and spatial future trends in precipitation and temperature variation in the largest fully developed basin in Greece (Pinios River Basin, PRB) and,
- To relate those changes to potential impacts in future water resources availability.

Given the fact that agriculture is the dominant water consumer in PRB accounting for over 90% of water use (Hellenic Ministry for the Environment, Energy and Climate Change-Special Secretariat for Water, 2014), precipitation and temperature evolution are expected to significantly affect water resource availability in the form of effective precipitation and crop water demands and indirect availability in the form of groundwater recharge and surface runoff.

Materials and methods

Study area description

PRB is located in Central Greece and covers an area of about 11,000 km^2. It is characterized by highly diversified geological, hydrological and hydrogeological conditions and marked by the systematic exploitation of water resources since early 1960s. From the water administration point of view, PRB belongs to the Thessaly water district (EL08) and covers the major part of this district (85%). Two climate types are identified in PRB: continental climate conditions are dominant at the central and western part of PRB, while typical Mediterranean climate conditions are met at the eastern part. For the period 1981–2000, the minimum average annual precipitation was 392 mm at the southeastern plain part of the basin, while the corresponding maximum value was 1705 mm at the western mountainous part. The average annual precipitation for the aforementioned period was 700 mm.

The agriculturally used plains covering 45% of PRB belong to the most intensively cultivated and productive agricultural areas of Greece. Accordingly, agriculture constitutes the major water consumer for Pinios river basin, since about 93% of total water consumption (1292 hm^3) is allocated to irrigation followed by domestic water supply (5.5%), livestock (1%) and industry (0.5%). According to Loukas (2010), a wide variety of crops are cultivated in PRB, including cotton, wheat, alfalfa and maize in the plain area, whereas apple, apricot, cherry, olive trees and grapes are cultivated at the foothills of the eastern mountains.

Permeable geological formations are dominating in PRB, since they cover about 44% of the total basin area. Impermeable geological formations and karstic aquifers cover about 40 and 16% of the total basin area, respectively. With regard to the hydrogeological conditions presented in PRB, the aquifers developed in quaternary depositions are indicating significant water abstraction potential followed by karstic aquifers found mainly around the plain parts of PRB. Since about 65% of total water consumption is satisfied by local aquifers, groundwater constitutes a vital water source for PRB.

In the framework of implementing EU-Water Framework Directive (EU-WFD, 2000), 27 groundwater bodies have been delineated in PRB, from which 3 display bad qualitative status because of high NO_3 concentrations attributed to agricultural activities. 9 groundwater bodies display bad quantitative status, i.e. declining groundwater tables, due to over-abstraction of groundwater for satisfying the agricultural irrigation needs.

The average long-term annual water discharge of PRB comprises 3300 hm^3. For assessing and documenting the status of surface waters of PRB, 73 river water bodies have been identified. As Pinios River surface waters are only used locally for feeding irrigation needs, 57 are characterized by low river water abstraction, 7 by medium water abstraction and only 9 by high water abstraction. In terms of pollution, Pinios river water quality is stressed by the discharge of treated and untreated domestic and industrial effluent and agricultural return flows (Loukas 2010). According to the recently revised water management plan, in terms of nitrogen loads and BOD, inputs from non-point (diffuse) sources are dominating (70 and 82% of the total loads, respectively), while concerning P, 32% of the total loads are attributed to non-point sources.

Climate data–bias-correction

Monthly precipitation data were collected from 57 meteorological stations located in the wider PRB area covering the period 1981–2000 (control period). For 17 of the 57 meteorological stations, average monthly temperature for the control period was also available. The location of the meteorological stations is illustrated in Fig. 1.

Despite the fact that output of GCMs has been widely applied in climate change assessment studies, the complexity of climate characteristics of Greece and its controlling factors cannot be adequately represented by GCMs (Tolika et al. 2012) and, therefore, the application of RCMs which are based on finer grid resolutions are thought more appropriate. Consequently, precipitation and temperature data were extracted from the ENSEMBLES project, in which state-of-the-art RCMs were used to produce regional simulations at a 25 or 50 km resolution (van der Linden and Mitchell 2009). These regional simulations are driven by ERA40 reanalysis data for the control period and by several GCMs under SRES A1B socio-economic scenario. Among the various models of ENSEMBLES project, data for the periods 1981–2000 and 2021–2100 were used from the following four RCMs: (a) HIRHAM5 (Christensen et al. 2006) driven by ARPEGE GCM (hereafter referred as HA), (b) RACMO2 (van Meijgaard et al. 2008) driven by ECHAM5 GCM (hereafter referred as RAE), (c) REMO (Jacob 2001) driven by ECHAM5 GCM (hereafter referred as REE) and (d) RCA (Kjellström et al. 2005) driven by HadCM3 GCM (hereafter referred as RH). These models were found to have sufficient performance in representing precipitation and temperature in several Mediterranean basins when compared to observed data (Deidda et al. 2013).

To improve local climate variability representation on regional and local assessment of climate change effects, further bias-correction in RCM output may be applied. A wide range of bias-correction methods are proposed in the scientific community, out of which the simple methods have the advantage of altering the RCMs' results as little as possible (Graham et al. 2007). The advantages and disadvantages of the most widely applied simple bias-correction methods, namely the delta change and linear scaling, are presented by Teutschbein and Seibert (2013). Linear scaling was applied for the purposes of this study, which has been previously used in several studies for the assessment of climate change impacts at river basin scale (Bosshard et al. 2013; Fiseha et al. 2014).

With regard to precipitation, a scaling factor was calculated for each calendar month, RCM and meteorological station as the ratio between the average observed and average simulated monthly precipitation for the period 1981–2000. Those scaling factors were subsequently multiplied by monthly precipitation data for the period 2021–2100 (2021–2099 for RH) for each calendar month. Monthly temperature was similarly corrected except that addition of a scaling factor to projected monthly average temperature was used, rather than multiplication.

The ordinary Kriging algorithm was applied to develop the spatial distribution of precipitation and temperature data in PRB. The period 2021–2100 was divided into four sub-periods of 20 years each to assess future trends in precipitation temporal variation. The results were analyzed on monthly, seasonal and annual basis for the four periods and compared to the corresponding precipitation and temperature data of the period 1981–2000, which will be referred to as historical period.

To assess RCM performance on representing precipitation and temperature variation patterns, as well as the performance of bias-correction, Taylor diagrams (Taylor 2001) were compiled, since they provide an efficient graphical method to present how well simulated patterns match

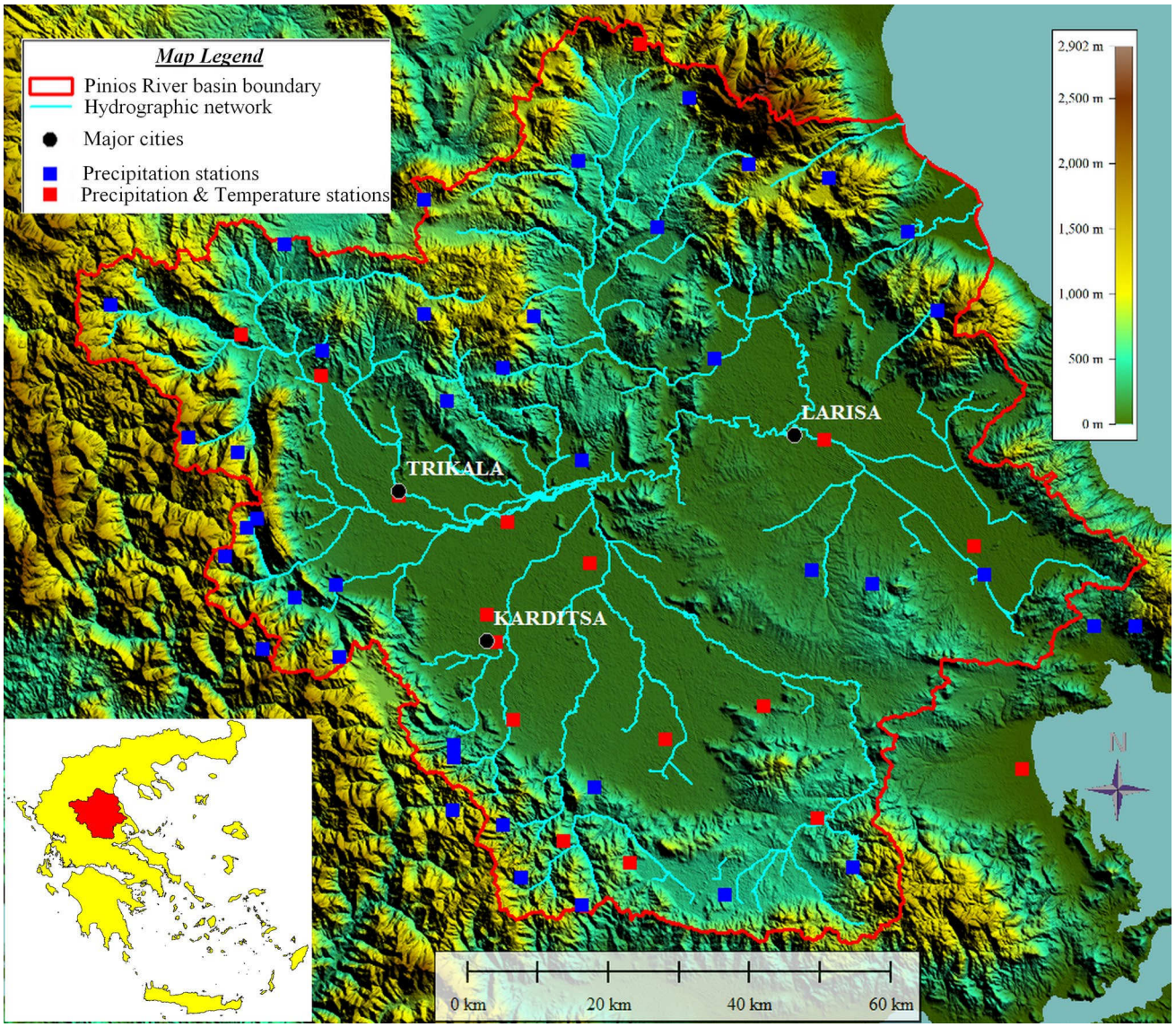

Fig. 1 Location map of the study area

the observed ones. Taylor diagrams are incorporating correlation coefficient, centered root mean square difference (cRMSD) and standard deviation into a single diagram and, therefore, they provide a clear overview of similarity between simulated and observed data.

Results

Future trends in precipitation variation

The Taylor diagram compiled by raw and bias-corrected RCM precipitation data for the period 1981–2000 is presented in Fig. 2. Points that are found closer to the "observed" quadrant of standard deviation and demonstrate higher correlation indicate better representation of observed patterns. With regard to raw RCM precipitation data, correlation coefficient ranged between 0.21 (REE) and 0.37 (RH), while standard deviation ranged between 1.35 (REE) and 2.02 mm/day (HA). The corresponding range for cRMSD was 2.26 mm/day (RH) to 2.53 mm/day (HA). Better performance is presented by RH and HA, since the first RCM indicates the highest correlation coefficient value and the latter indicates standard deviation closer to the observed one. All RCMs were found to underestimate standard deviation and, therefore, they indicate lower precipitation variation compared to the observed. The bias-correction procedure improved correlation coefficient since it was found to be increased by more than 0.1 units for all RCMs (0.39–0.5), while significant improvement was also observed for

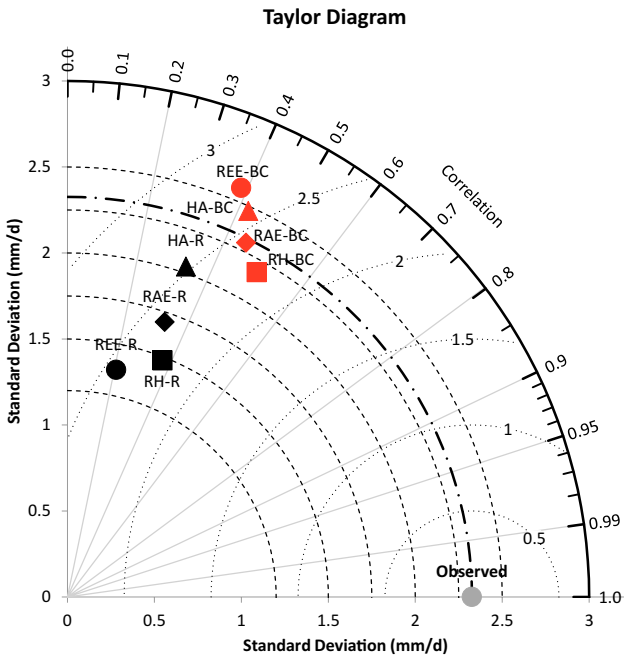

Fig. 2 Taylor diagram of raw (R) and bias-corrected (BC) RCM precipitation data for the period 1981–20

standard deviation for all RCMs. RH and RAE RCMs indicate better performance after bias-correction application.

Annual precipitation temporal variation was assessed for the four sub-periods and compared to the median total annual precipitation of historical period (1981–2000), which is 682 mm (or 7500 hm^3) and the results are illustrated in Fig. 3. A wide range of annual precipitation change is indicated for all RCM–GCM combinations and all periods. The general point of the results illustrated in Fig. 3 is that precipitation is expected to be significantly decreased, especially during the period 2041–2060. Climate change signal for the period 2021–2040 is not very clear as highly controversial estimates are generated; HA indicates a very significant decrease of precipitation by 166 mm on the median, while RAE also indicates annual precipitation decrement by 52 mm. REE and RH present annual precipitation increment by 6 and 82 mm on the median, respectively. According to RH results, precipitation is also increased for the period 2041–2060 by 97 mm on the median, while the other RCM–GCM combinations indicate significant decrease in precipitation ranging between − 136 mm (RAE) and − 116 mm (HA). For HA, RAE and REE precipitations are further decreased during the period 2061–2080 (− 197 to − 131 mm), while for RH, precipitation was found to be increased by 15 mm. Finally, for the period 2081–2100 (2099 for RH) precipitation decreases for all models and the decrement ranges between − 261 and − 68 mm. On the average, the highest annual precipitation decrease for the period 2021–2100 is demonstrated by HA (149 mm or 1647 hm^3), followed by RAE (113 mm or 1.250 hm^3) and REE (− 91 mm or 1007 hm^3), while RH results indicate a small increase in average total annual precipitation for the period 2021–2099 (35 mm or 391 hm^3). Increased precipitation for the period 2011–2100 is also indicated by RH for Vosvozis river basin located in northeastern Greece (Pisinaras et al. 2014).

When comparing the temporal change of annual precipitation for each RCM–GCM model combination, different trends are indicated. HA demonstrates a very significant decrease during 2021–2040, which becomes milder but still significant during 2041–2060. In contrast, RAE demonstrates a very small precipitation decrease during 2021–2040, while for the period 2041–2060 precipitation decrease is much more significant and almost equal to precipitation decrease for the period 2061–2080. REE temporal variation is similar to RAE except from the period 2081–2100, during which precipitation decrease is lower when compared to precipitation decrease for the periods 2041–2060 and 2061–2080. The increased precipitation indicated by RH in the present study has been also indicated by Tolika et al. (2012) for precipitation projection with RCA-ECHAM4.

The spatial distribution change of annual total precipitation for the period 2021-2100 for each RCM–GCM combination is presented in Fig. 4. Similar trends of precipitation spatial distribution change are presented for HA, RAE and REE, as higher precipitation decrease is deduced for the mountainous parts of the PRB and especially for its eastern part. In contrast, RH indicates increased precipitation in the mountainous parts of PRB and decreased precipitation in the central plain part.

To identify temporal trends in precipitation variation on seasonal basis, box-plots of seasonal total precipitation were created for all sub-periods and RCM–GCM combinations, which are presented in Fig. 5. In general, there are some clear variation trends identified when the seasonal precipitation for the period 2021–2100 is compared to the historical period, but seasonal precipitation variation within the four sub-periods appears complex, as there is no continuous and stable trend observed for each model. For example, according to HA results, median autumn precipitation is presented to be 166 mm for the period 2021–2040, increases to 177 mm during the period 2041–2060, decreases to 166 mm during the period 2061–2080 and finally increases to 183 mm during the period 2081–2100.

Concerning the autumn season, there is a general trend observed which indicates wider seasonal precipitation variation range and subsequently increment in precipitation extremes, either low or high. The high autumn precipitation extremes are increasing the potential negative impact on agricultural production for crops such as cotton, which is the dominant crop for PRB and its cultivation period usually

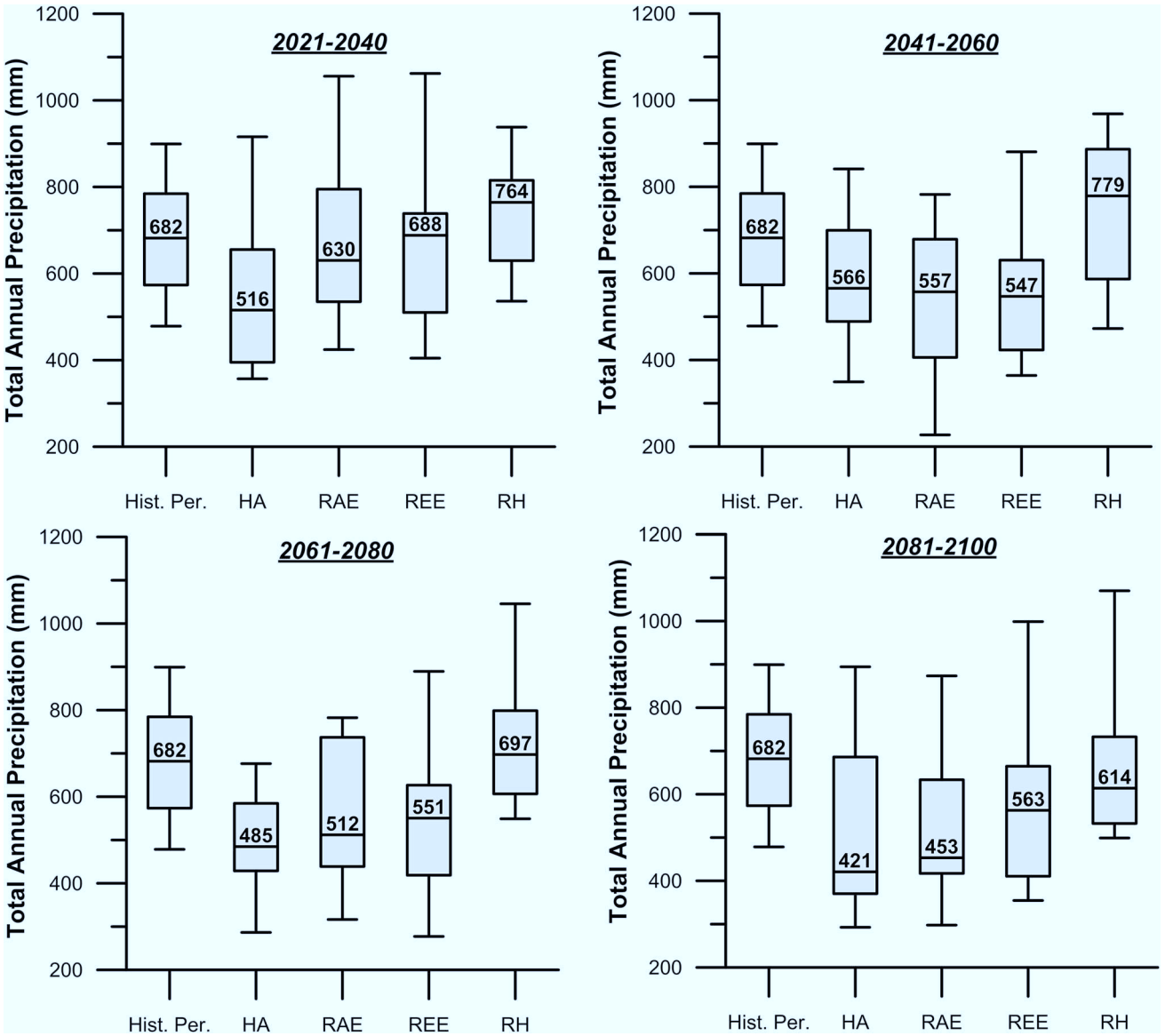

Fig. 3 Box-plots of total annual precipitation variation according to results from the four RCM–GCM combinations for the periods 2021–2040, 2041–2060, 2061–2080 and 2081–2100

ends between end of October and middle November. RAE and REE indicate increased autumn precipitation by 20 and 30 mm, respectively, during the period 2021–2040, significantly decreased values during the periods 2041–2060 and 2061–2080, and slightly increased precipitation values during the period 2081–2100, compared to the corresponding precipitation values for the historical period. HA and RH indicate decreased autumn precipitation compared to the historical period for all the sub-periods, while the highest autumn precipitation decrement is presented by RH for the period 2081–2100 and it is equal to 69 mm.

Except from RH, the other three RCM–GCM combinations indicate a decreasing trend in winter precipitation for all the sub-periods, with the overall strongest decreasing trend indicated by HA ranging between 16 mm (sub-period 2041–2060) and 80 mm (sub-period 2061–2080). RH presents decreased winter precipitation only for the period 2081–2100 and increased winter precipitation for the other three sub-periods. Similarly to autumn season, there is a general trend according to which winter precipitation variation range is wider compared to the corresponding variation range of the historical period, thus indicating increment in precipitation extremes, either low or high, for most of the examined model combinations and sub-periods.

Concerning spring precipitation variation and similarly to autumn precipitation, HA, RAE and REE models indicate

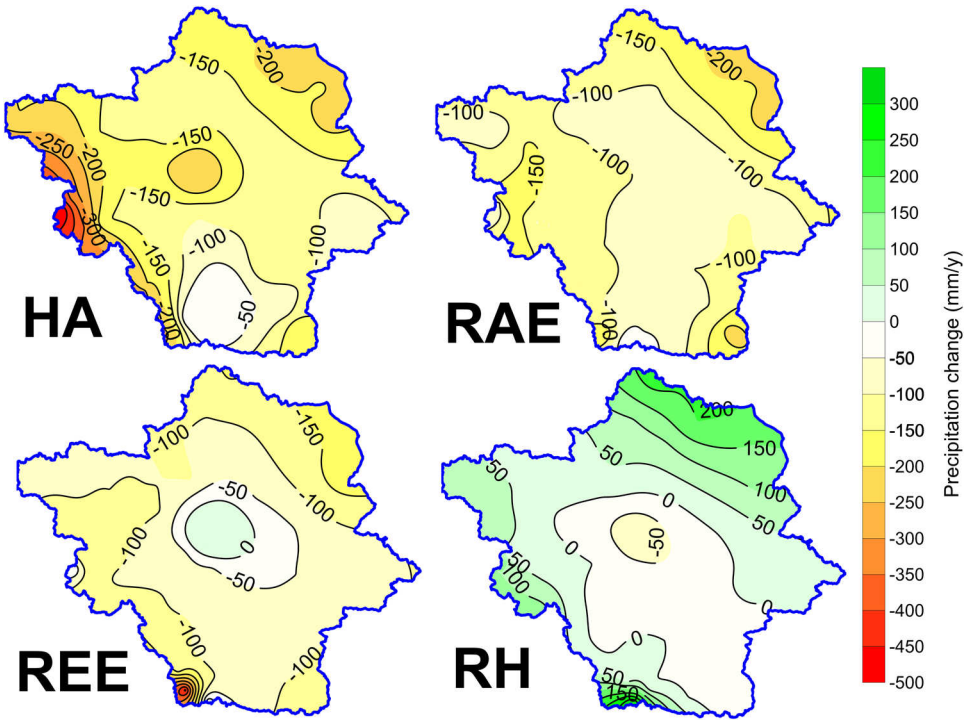

Fig. 4 Spatial distribution of average annual total precipitation change for the period 2021–2100 for each RCM–GCM combination

decreasing trend for all sub-periods, with the overall strongest decreasing trend indicated by HA ranging on the median between 66 mm (period 2041–2060) and 99 mm (period 2081–2100). For the periods 2021–2040 and 2041–2060, spring season precipitation according to RH model is presented slightly increased by 6 and 2 mm, respectively, while for the periods 2061–2080 and 2081–2100 is presented as decreased by 19 and 10 mm, respectively, compared to the spring precipitation of the historical period. In contrast to autumn and winter, the variation and inter-quartile range presented by the RCM–GCM combinations during the several sub-periods are similar to the variation and inter-quartile range of the historical period.

Finally, summer precipitation variation follows the general trends observed for winter and spring, however, exhibiting wider seasonal variation range. Hence, it decreases for all sub-periods and RCM–GCM combinations, except from RH. The summer precipitation decrement ranges on the median between: (a) 21.6 and 48.5 mm for the period 2021–2040, (b) 20.9 and 46.5 mm for the period 2041–2060, (c) 27.3 and 55.3 mm for the period 2061–2080 and (d) 37.6 and 56.2 for the period 2081–2100. For RH, median value of summer precipitation is increased compared to that of the historical period. Moreover, compared to autumn and winter, summer precipitation indicates increased seasonal precipitation variation range, while total dry summer periods are also demonstrated by the models HA, RAE and REE.

In complement to annual and seasonal precipitation variation, monthly precipitation variation was also assessed. The cumulative frequency diagrams for the four sub-periods and for each RCM–GCM combination are presented in Fig. 6. These diagrams indicate that at least one RCM–GCM combination indicates maximum monthly precipitation greater than the corresponding maximum of the historical period and, therefore, increment in monthly precipitation extremes is presented by most of the RCM–GCM combinations. This is also proved from the fact that for cumulative frequency values > 90%, higher precipitation values are indicated for most RCM–GCM combinations and sub-periods. For cumulative frequency values < 90%, HA, RAE and REE are presenting lower monthly precipitation for all the sub-periods, while the strongest decreasing precipitation signal is presented for the sub-period 2081–2100. RH indicates significantly different variation patterns, as for cumulative frequency values < 80% it presents monthly precipitation values which are close to or greater than the corresponding values of the historical period.

Future trends in temperature variation

The Taylor diagram compiled by the raw and bias-corrected RCMs temperature data for the period 1981–2000 is presented in Fig. 7. Points that are found closer to the "observed" quadrant of standard deviation and demonstrate higher correlation indicate better representation of observed patterns. With regard to raw RCM temperature data, correlation coefficient ranged between 0.962 (REE) and 0.972 (RAE), while standard deviation ranged between

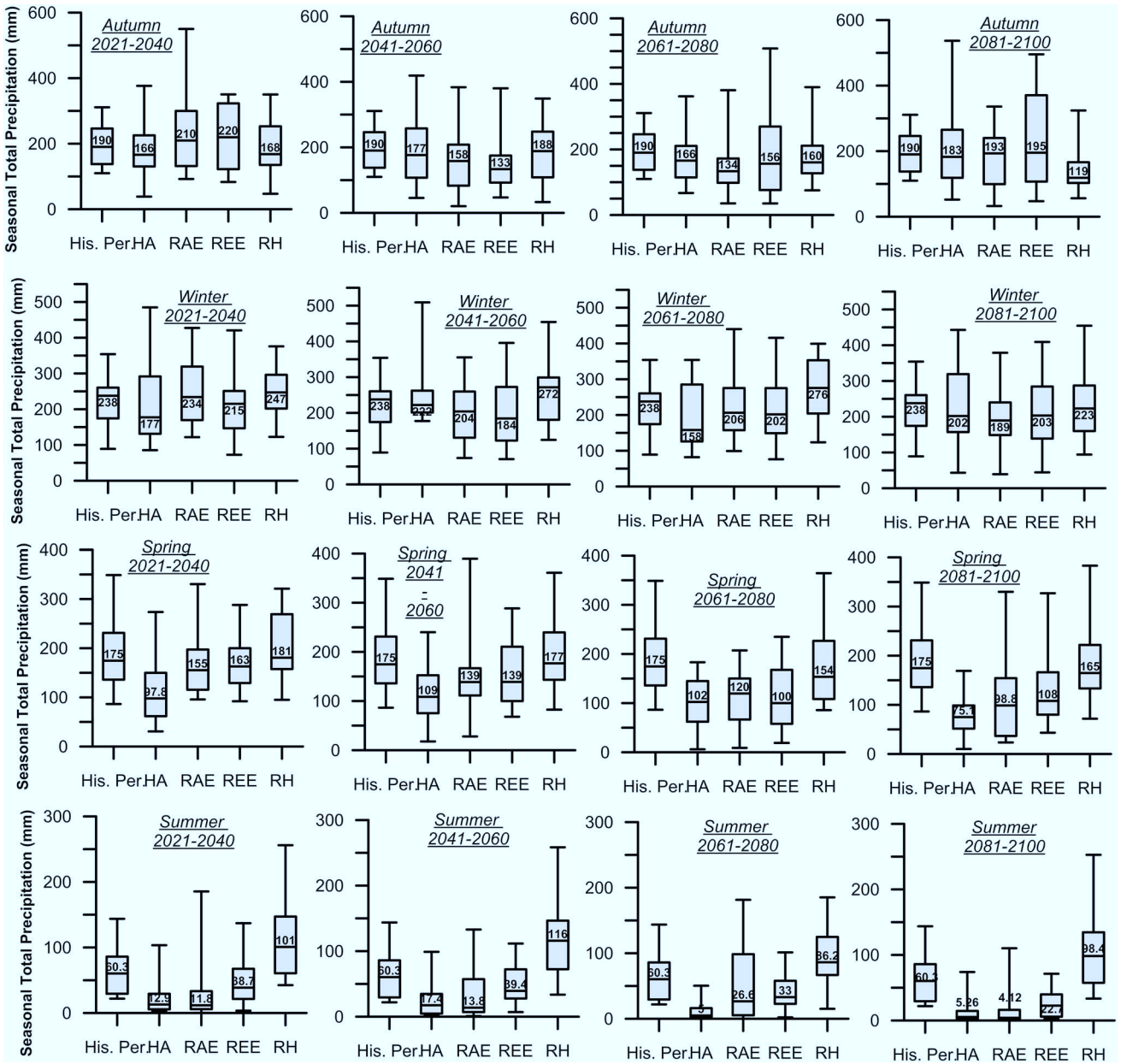

Fig. 5 Box-plots of seasonal total precipitation variation according to results from the four RCM–GCM combinations for the periods 2021–2040, 2041–2060, 2061–2080 and 2081–2100

7.96 (HA) and 8.53 °C (REE). The corresponding range for cRMSD was 2.05 °C (RH) to 2.3 °C (REE). Since correlation coefficient values of all RCMs raw temperature data are similar, the best performance is presented by RH since it indicates standard deviation closer to the observed one. All RCMs were found to slightly overestimate standard deviation and, therefore, they indicate higher temperature variation compared to the observed. The bias-correction procedure improved correlation coefficient since it was found to be increased by more than 0.02 units for all RCMs (0.983–0.987), while improvement was also observed for standard deviation for all RCMs. After bias-correction, all RCM performance was found to be similar.

Average annual temperature variation for the four sub-periods is presented in Fig. 8. Despite the fact that all RCM–GCM combinations are indicating temperature increase during the period 2021–2100, the variation range of temperature increase produced by each RCM–GCM is large. Still, clearer trends are depicted for all tested models combinations, compared to the afore-discussed precipitation trends. Depending on the period, the highest temperature increment is indicated by a different model. For the periods

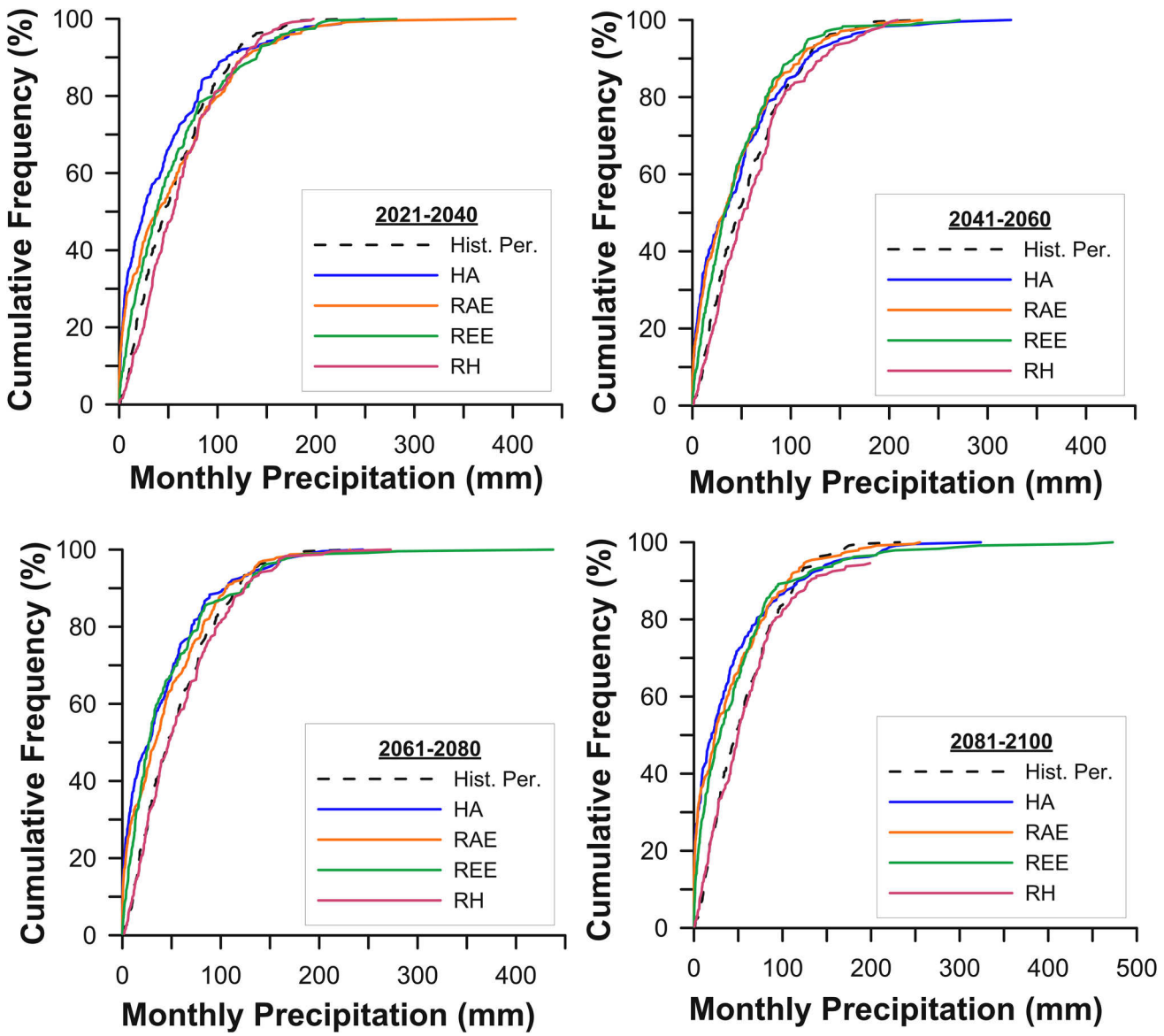

Fig. 6 Cumulative frequency diagrams of monthly precipitation for the historical period (1981–2000) and all RCM–GCM combinations at the four sub-periods

2021–2040 and 2041–2060, the highest temperature increase is indicated by HA, while for the periods 2061–2080 and 2081–2100 the highest temperature increase is presented by RAE. The lowest temperature increase is demonstrated for the whole projection period by RH model. For the period 2021–2040, the temperature increase ranges between 0.2 °C (RH) and 3.3 °C (HA), while the corresponding range for the period 2041–2060 is 1.3 °C (RH) and 3.7 °C (HA). For all RCMs–GCMs, temperature is projected to further increase during the period 2061–2080 [2 (RH) to 4 °C (RAE)], while the highest temperature increase is presented for all models during the period 2081–2100 (2081–2099 for RH) ranging between 2.6 (RH) and 5.1 °C (RAE). The comparison of temporal change of temperature for each RCM–GCM models combination indicates almost linear temperature increment for RAE, REE and RH, while for HA, temperature increase for the period 2041–2060 is almost equal to the temperature increase for the period 2061–2080.

Moreover, similarly to temperature variation for most seasons, it is worth mentioning that especially for HA, RAE and REE the minimum average annual temperature is higher than the maximum average annual temperature observed during the historical period, thus indicating significant difference in annual temperature variation pattern. Even for RH results which indicate the weakest climate change signal, the inter-quartile ranges of annual temperature variation for

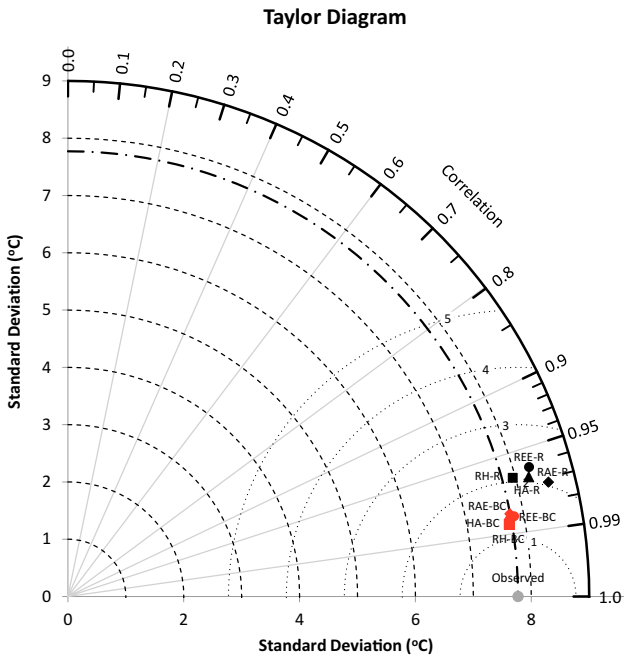

Fig. 7 Taylor diagram of raw (R) and bias-corrected (BC) RCM temperature data for the period 1981–2000

the periods 2041–2060, 2061–2080 and 2081–2100 do not overlap with the corresponding inter-quartile range of the historical period.

The spatial distribution of average annual temperature change for the period 2021–2100 for each RCM–GCM combination is illustrated in Fig. 9, in which significant differences are illustrated. HA and RAE present a smooth spatial distribution of temperature gradient, which is higher in the mountainous part of the basin, while REE demonstrates a highly contrasting spatial distribution with significantly higher temperature gradient in the mountainous part of PRB. In contrast, RH demonstrates lower temperature increase in the mountainous part than temperature increase in the plain part.

With regards to seasonal average temperature variation, box-plots for the results of all RCM–GCM combinations and the four sub-periods were created and compared to the results of historical period (Fig. 10). Except from RH autumn temperature for the period 2021–2040 which is estimated to be decreased compared to the historical period, all the other models demonstrate increased seasonal temperature for all periods and all seasons. Concerning autumn, the overall strongest climate change signal is on the median presented by HA with temperature increment ranging between 3.2 (sub-period 2021–2040) and 4.5 °C (sub-period 2081–2100). Moreover, it is interesting to mention that according to HA results, minimum median autumn temperature is higher than the maximum median autumn temperature observed during the historical period, thus indicating significant difference in autumn temperature variation pattern. This is also indicated by RAE and REE results, according to which their inter-quartile range does not even partially overlap with the corresponding inter-quartile range of the historical period. Significantly different variation pattern is presented by RH results, for which autumn temperature illustrates milder increment ranging between 0.6 (sub-period 2041–2060) and 1.8 °C (sub-period 2081–2100).

In terms of winter temperature variation, the overall strongest climate change signal is indicated by RAE model, which illustrates, on the median, temperature increment that ranges between 2.5 (sub-period 2021–2040) and 5.4 °C (sub-period 2081–2100). Significant winter temperature increase is also presented by HA (3.1–4.2 °C) and REE (1.7–4.4 °C). The lowest winter temperature increase is illustrated by RH and ranges between 0.7 (sub-period 2041–2060) and 2.1 °C (sub-period 2081–2100), while wider temperature variation ranges are demonstrated for all periods. Similarly to autumn temperature, the inter-quartile variation ranges for the models HA, RAE and REE, and the whole 2010–2100 period does not overlap with the corresponding range of the historical period, thus indicating significant difference in winter precipitation patterns. Compared to autumn and winter, spring average temperature indicates lower but significant increase compared to the historical period. Spring temperature is constantly increasing during the period 2021–2100 and the corresponding increment ranges for the four RCM–GCM combinations are 2.3–3.2 °C (HA), 1.8–4.4 °C (RAE), 0.3–3.2 °C (REE) and 0.6–2.5 °C (RH).

Considering that PRB is dominated by summer crops, any changes in summer temperature variation can potentially affect agricultural production. Among the four seasons, summer presents the strongest climate change signal with temperature increment on the median by up to 5.9 °C. More specifically, the overall higher temperature increment is presented by HA (3.8–5.5 °C) followed by RAE (2.1–5.9 °C) and REE (1.4–4.9 °C), while the lowest temperature increment is presented by RH (0.8–3.4 °C). Similarly to spring, summer temperature is steadily increasing during the period 2021–2100 for all RCM–GCM combinations, while the significant differences in variation range and inter-quartile ranges indicate the important differences in temperature variation patterns.

Similarly to precipitation, cumulative frequency diagrams of average monthly temperature for the four sub-periods and for each RCM–GCM combination are presented in Fig. 11. Concerning the sub-period 2021–2040, the widest monthly temperature variation range is presented by RH, according to which minimum monthly temperature expected to be observed during the period 2021–2040 is much lower than the corresponding temperature observed during the historical period. The other three models demonstrate higher minimum monthly temperatures. The strongest climate change

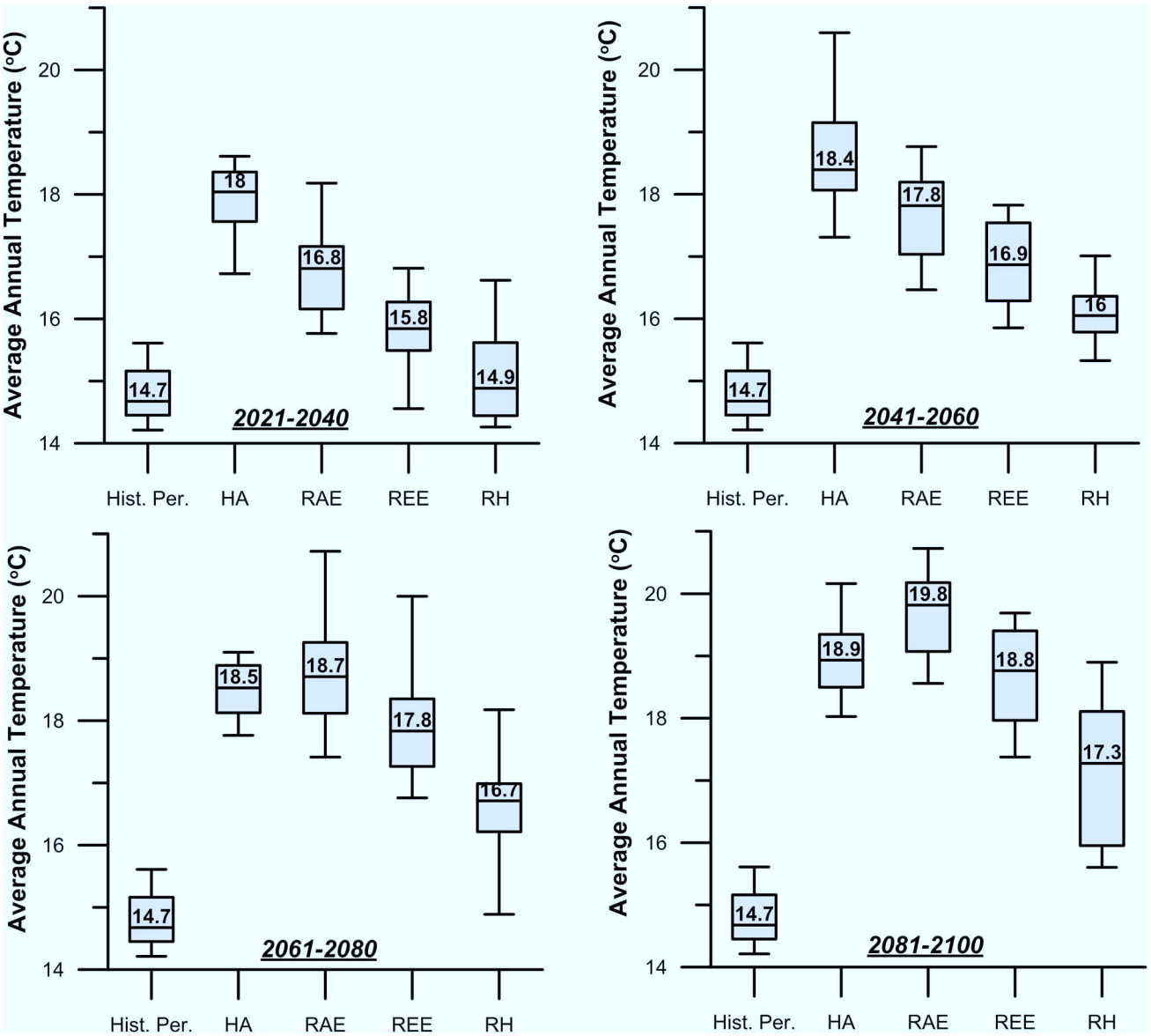

Fig. 8 Box-plots of average annual temperature variation according to results from the four RCM–GCM combinations for the periods 2021–2040, 2041–2060, 2061–2080 and 2081–2100

signal is presented by HA due to the fact that monthly temperature is higher for the whole range of cumulative frequency curve, followed by RAE. The lowest climate change signal is demonstrated by RH, as the cumulative frequency curve for RH is very close to the corresponding curve of the historical period, except from cumulative frequency values > 0.9 for which significantly higher monthly temperature values are indicated by RH compared to the historical period. The cumulative frequency curves for the other three sub-periods presented in Fig. 11 are shifting steadily to the right, thus indicating further increment in average monthly temperature compared to the historical period. Moreover, it is worth noting that despite the fact that for cumulative frequency values < 0.4 during the period 2081–2100 there are noticeable differences between the cumulative frequency curves, for cumulative frequency values > 0.4 the differences are smoother; hence lower inter-model variability is presented for low monthly temperatures compared to high temperatures.

Discussion

Clearly, precipitation and temperature are crucial parameters in shaping water budget, especially so under climate change conditions in an intensively cultivated basin, such

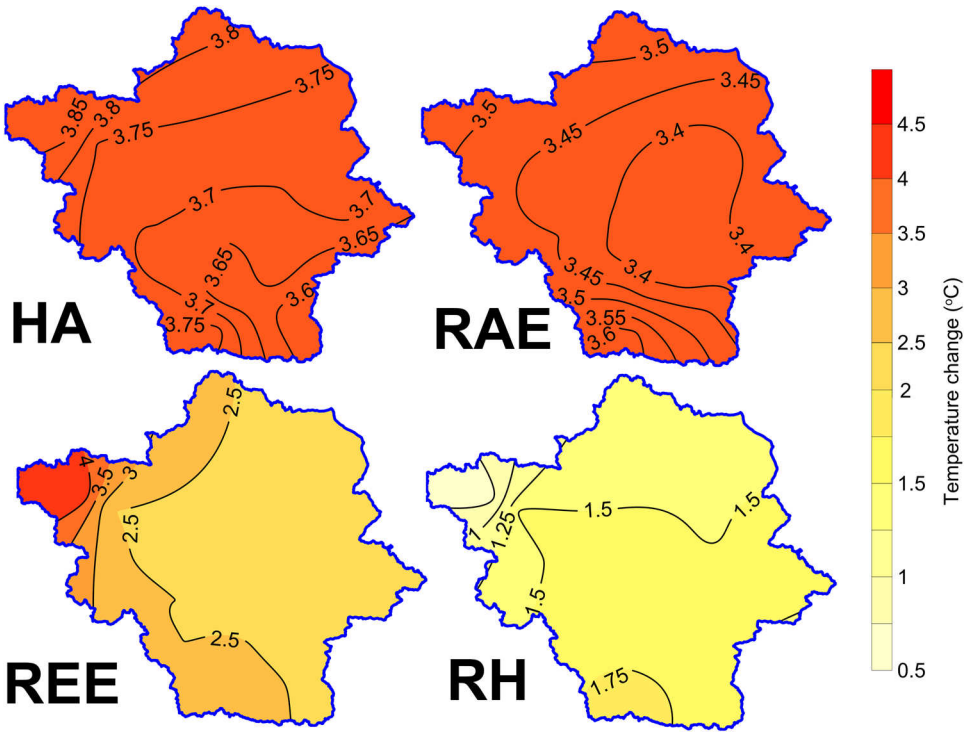

Fig. 9 Spatial distribution of average annual temperature change for the period 2021–2100 for each RCM–GCM combination

as PRB. Hence, the presented results of the estimated shift in precipitation and temperature patterns are expected to considerably affect future water resource availability and status. PRB has been found to be severely stressed in terms of its water resources, since the last few decades (Koutsoyiannis and Mimikou 1996; Loukas et al. 2007). The major responsibility for water resource stress developed in PRB is the agricultural sector, as irrigation water consumption accounts approximately for 95% of the total water consumption (Koutsoyiannis and Mimikou 1996; Alexandridis et al. 2014). Although there are studies which indicate that the annual water availability is higher than the corresponding water needs (Koutsoyiannis and Mimikou 1996), the high demand for irrigation water during the summer cultivation period leads to groundwater over-exploitation, as surface water availability during this period is low. Therefore, about 80% of irrigation water needs are covered by groundwater abstracted mainly from aquifers developed in the plain areas of PRB. The huge number of productive wells in PRB, which is estimated to exceed 30,000 (Hellenic Ministry for the Environment, Energy and Climate Change-Special Secretariat for Water 2014), is indicative of the groundwater over-exploitation conditions developed in the basin. Panagopoulos et al. (2012) indicate that water-deficient budget conditions have already been established in several water systems of the studied basin. According to Loukas et al. (2007), some proposed surface water storage projects would significantly contribute to the reduction of PRB water deficit without being able to satisfy total water needs. Not even the partial diversion of the Acheloos River, located in central–western Greece, into PRB will be able to account for the negative water balance during dry hydrological years.

Since RCMs have been found to partially reproduce climate pattern in Europe (Jacob et al. 2007; Christensen and Christensen 2010) and taking into account the regional character of our study, we decided to include in our study RCMs that have been proved in the literature to reproduce satisfactorily climate patterns in Mediterranean conditions. The four RCMs selected in the context of the present study have been found to sufficiently represent precipitation and temperature variation in several Mediterranean basins when compared to observed data (Deidda et al. 2013), while they are also introducing a significant degree of variation both for precipitation and temperature.

Overall, the strongest signal taken from projected climate data is precipitation decrease and temperature increase, since annual precipitation change for the period 2021–2100 was on the average about − 80 mm (or − 11.7%, 883 hm^3), ranging between − 149 (or − 21.8%, 1644 hm^3) and + 35 mm (or 5%, 386 hm^3), while the corresponding change for temperature was 2.81 °C, ranging between 1.48 and 3.72 °C. Despite the different periods examined, the aforementioned trends are similar to previous studies for PRB and central–eastern Greece. Zanis et al. (2009) assessed the projected future precipitation and temperature change (2071–2100) using the PRUDENCE dataset consisting of nine RCMs and they estimated for central–eastern Greece an annual precipitation decrease by 15.5% and an average annual temperature

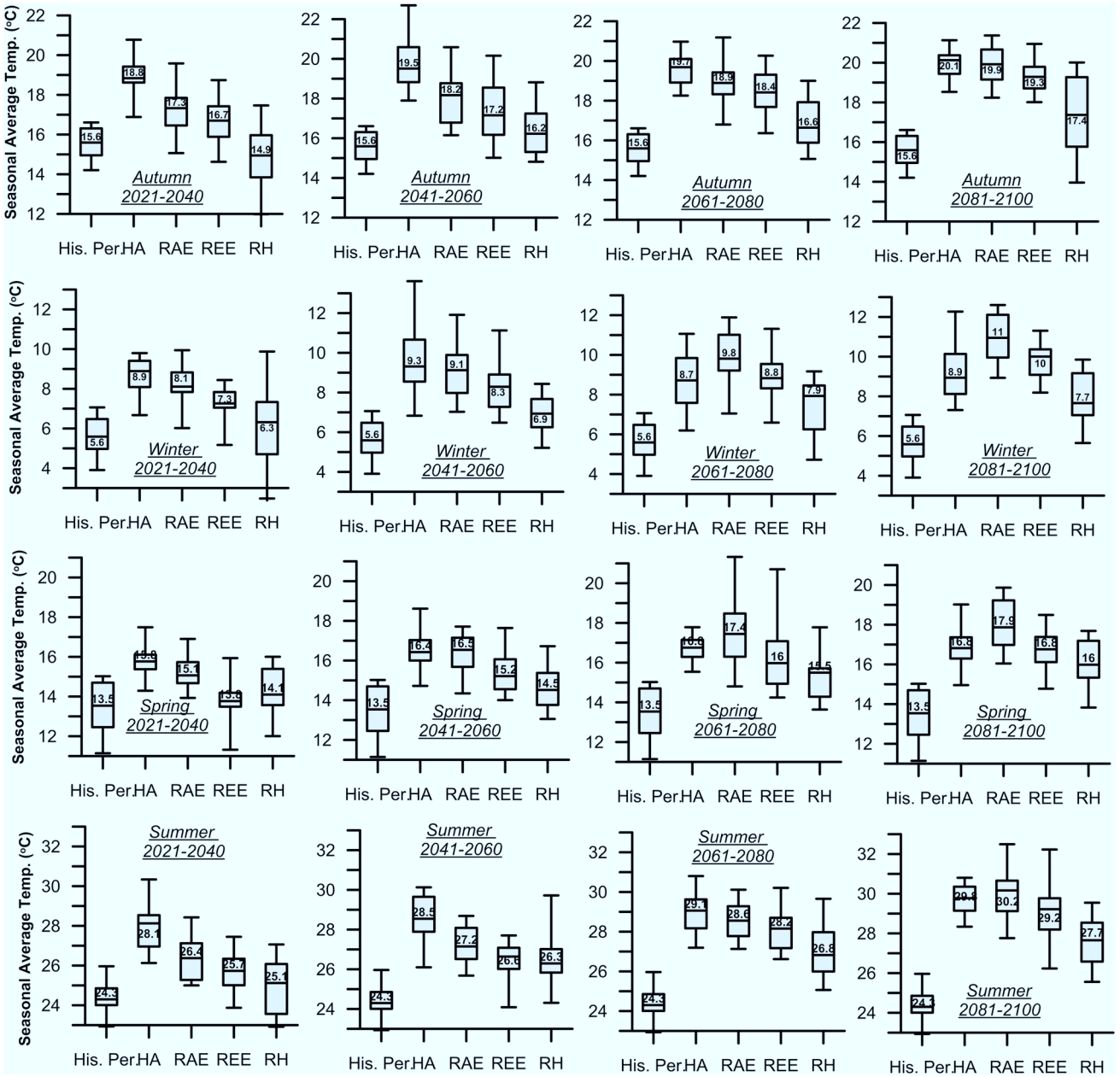

Fig. 10 Box-plots of seasonal average temperature variation according to results from the four RCM–GCM combinations for the periods 2021–2040, 2041–2060, 2061–2080 and 2081–2100

increase by 4.0 °C. According to Vasiliades et al. (2009), an average annual precipitation reduction of about 3.9 and 3.4% for period 2020–2050, and of about 13.5 and 8.5% for period 2070–2100 for SRES A2 and SRES B2, respectively, was estimated based on downscaled precipitation data from CGCMa2 model. According to Mimikou et al. (2000), precipitation decrease and temperature increase were indicated by two GCMs used to quantify the effects of climate change in a sub-basin of PRB (Ali Efenti). Varanou et al. (2002) used precipitation and temperature data from four GCMs concluding that decreasing trend is dominant in precipitation variation, while temperature increase was suggested for all scenarios and models. Compared to these studies, the here presented trends have been evaluated based on RCM data, indicating higher resolution than GCMs, which was further bias-corrected, thus representing a higher local representativeness.

When aggregating precipitation data from the four RCMs for the four future periods and comparing to the period 1981–2000, winter precipitation decrease ranges between 7.2% (period 2041–2060) and 14.0% (period 2081–2100) and temperature increase ranges between 2.06 (period

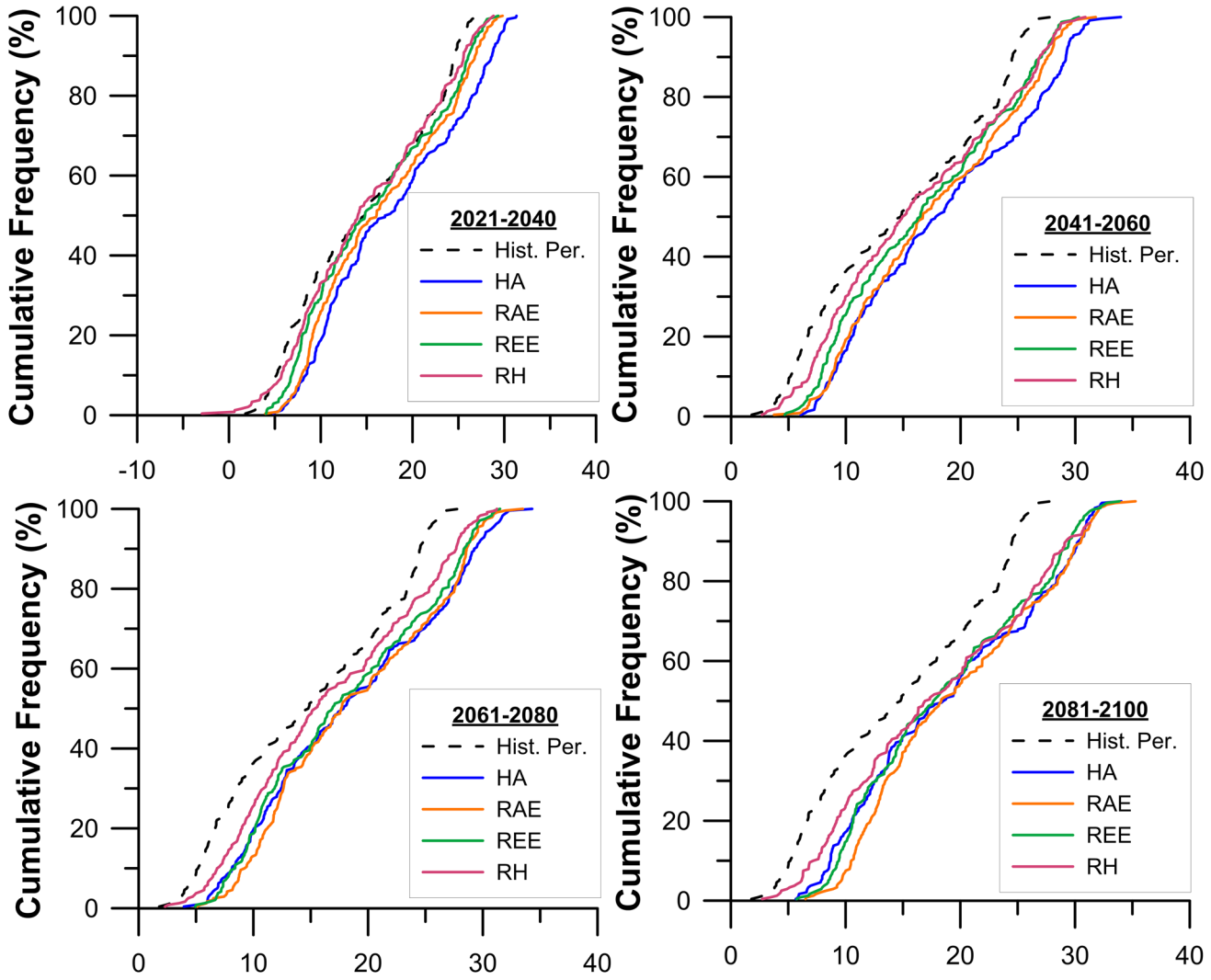

Fig. 11 Cumulative frequency diagrams of average monthly temperature for the historical period (1981–2000) and all RCM–GCM combinations at the four sub-periods

2021–2040) and 3.80 °C (period 2081–2100). The corresponding changes for central–eastern Greece presented by Zanis et al. (2009) based on PRUDENCE dataset consisting of nine RCMs for winter of period 2071–2100 and A2 scenario are − 20.4% for precipitation and 3.70 °C for temperature. Taking into account that the winter season is the wettest period for PRB with the lowest evapotranspiration amounts, it is significantly contributing to the replenishment of water consumed during the irrigation period through groundwater recharge or through the collection of surface runoff in the dams. Moreover, rainfed crops such as wheat, which cover significant parts of PRB, are cultivated during winter. Therefore, the decrement of winter precipitation and the corresponding increment in potential evapotranspiration is expected to significantly stress the availability of water resources during winter in two ways: (a) decrement in groundwater recharge and (b) increment in potential evapotranspiration not only for non-cultivated areas but also for winter crops, and consequently increased water needs. Finally, the increased variation and inter-quartile range presented for most of the future periods and RCMs constitute an indicator of increment in precipitation extremes, either low or high, and therefore increased risk for effective water resources management due to increased flooding potential (in case of high extremes) or droughts (in case of low extremes).

The corresponding precipitation decrease for spring during the period 2021–2100 ranges between 14.6 (period 2021–2040) and 36.1% (period 2081–2100), while temperature increase ranges between 2.1 (period 2021–2040) and 3.8 °C (period 2081–2100). Similarly to winter, early spring is a period of significant precipitation contribution to groundwater recharge and, therefore, precipitation decrement is expected to result in groundwater recharge decrement.

Moreover, spring period is very significant for the development of rainfed winter crops, the cultivation period of which usually ends at early summer and combined to potential evapotranspiration increase as a result of the increased temperature, the water stress of winter crops is expected to be increased. Moreover, spring season constitutes the sowing period for summer crops in PRB. Taking into account the elevated water needs indicated by temperature increase, in combination with reduced water availability as a result of precipitation decrease, the water stress indicated by summer crops during the spring period is significant.

Since agricultural activities and especially summer crops are dominating water consumption in PRB, summer precipitation is of high importance and the demonstrated decreasing trend ranging between 22.7 (period 2041–2060) and 45.9% (period 2081–2100) reflects the necessity for increased irrigation to satisfy water demand of the summer crops. Water demand is expected to further increase in response to temperature increase which ranges between 2.0 and 4.9 °C, as a result of the increased potential evapotranspiration. The corresponding changes for central–eastern Greece presented by Zanis et al. (2009) based on PRUDENCE dataset consisting of nine RCMs for summer of period 2071–2100 and A2 scenario are − 54.2% for precipitation and 5.00 °C for temperature. It has to be mentioned that crops that are not tolerant to the temperature increase will suffer from temperature stress, leading to decreased agricultural production, thus posing another risk except from water resource availability reduction. Concerning the autumn season, precipitation data aggregation from the four RCMs indicates that seasonal precipitation change may vary on average from − 19.0 (period 2061–2080) to 0.4% (period 2021–2040), while corresponding temperature increase ranges between 1.4 and 3.6 °C. Due to the fact that for the most significant crops cultivated in PRB, cultivation period extends to autumn, the significant change in autumn temperature variation can potentially increase water demand during early autumn and affect crop growth behavior.

Based on the overall results produced by the examined model combinations and taking into account that the reference period (1981–2000) includes a severe drought period (Loukas and Vasiliades 2004) which significantly affected the water balance of PRB, the anticipated effects of climate change in water resources availability and management are expected to be severe. The aforementioned trends are expected to lead to an acute water-deficit condition, since potential evapotranspiration shall increase (both for winter and summer crops) with parallel decrease of precipitation share to irrigation, and obviously effective precipitation for natural groundwater replenishment is expected to further decrease or even vanish over specific years and/or periods. Consequently, water demands will need to be catered for by either groundwater abstractions and/or further abstractions from surface water bodies, thus magnifying the water-deficient budget conditions that have already been established in PRB, as described above. Moreover, as deduced from the presented results, during the wet seasons and especially during winter, a high precipitation intensity variability is anticipated along with overall decrease in total precipitation heights that could potentially lead to: (a) increased flash flood events, (b) soil clogging effects, (c) decreased natural recharge of groundwater bodies. All three phenomena may trigger extensive soil erosion leading to desertification, magnification of existing or triggering of new groundwater depletion conditions (that may eventually lead to mining) and fresh water reserves pollution.

Conclusions and outlook

This study aimed to quantify the temporal and spatial variation in precipitation and temperature in PRB using bias-corrected data from four RCMs, driven by different GCMs for the emissions scenario A1B and relate this variation to potential impacts in water resources status and availability. Results of the study are in agreement with other studies in Mediterranean region that indicate decreasing trend in precipitation and increasing trend in temperature, despite the considerable differences in the spatial and temporal distribution of both parameters. The above-mentioned trends are expected to significantly affect the water availability in PRB in several ways, including mainly reduction in groundwater recharge and increase in irrigation demands. Taking into account that water balance in PRB is deficient already since 1990′s, the water stress signal becomes more intense and climate change adaptation becomes more difficult. This fact highlights the necessity of investigating climate change effects on the local scale to incorporate the specific and particular water resource management conditions. It would appear that crop patterns, irrigation methods and overall water management approaches need to be carefully considered and appropriately adapted to address forthcoming climate change effects. The expected climate changes effects call for optimal use and sufficient protection of water resources to endure impacts and ensure adequate volumes of sufficient quality.

The careful data evaluation as shown in this paper is indispensable to comprehend climate change impact on water resource availability and spatio-temporal distribution. Application of the presented climate change data shall be used in setting up mGROWA (Herrmann et al. 2015), a hydrologic model of high temporal and spatial resolution to assess the impact of climate change on development of water availability and the inner-annual shift of runoff generation periods for the entire basin. The results of such a model are deemed essential in developing an applicable and realistic

strategic management tool for water resources in the sensitive and complex environment of the Pinios River Basin.

Acknowledgements The authors thank and gratefully acknowledge the ENSEMBLES project, funded by the European Commission's 6th Framework Programme through contract GOCE-CT-2003-505539 for providing RCM climate data. We would like to gratefully thank the two anonymous reviewers for their time and effort in reviewing the article.

References

Alexandridis TK, Panagopoulos A, Galanis G, Alexiou I, Cherif I, Chemin Y, Stavrinos E, Billas G, Zalidis GC (2014) Combining remotely sensed surface energy fluxes and GIS analysis of groundwater parameters for irrigation system assessment. Irrig Sci 32(2):127–140

Bosshard T, Carambia M, Goergen K, Kotlarski S, Krahe P, Zappa M, Schär C (2013) Quantifying uncertainty sources in an ensemble of hydrological climate-impact projections. Water Resour Res 49(3):1523–1536

Chenoweth J, Hadjinicolaou P, Bruggeman A, Lelieveld J, Levin Z, Lange MA, Xoplaki E, Hadjikakou M (2011) Impact of climate change on the water resources of the eastern Mediterranean and Middle East region: modeled 21st century changes and implications. Water Resour Res 47:W06506

Christensen JH, Christensen OB (2010) A summary of the PRUDENCE model projections of changes in European climate by the end of this century. Clim Change 81:7–30

Christensen OB, Drews M, Christensen JH, Dethloff K, Ketelsen K, Hebestadt I and Rinke A (2006) The HIRHAM Regional Climate Model Version 5 (beta), DMI, Technical Report 06-17

Deidda R, Marrocu M, Caroletti G, Pusceddu G, Langousis A, Lucarini V, Puliga A, Speranza A (2013) Regional climate models' performance in representing precipitation and temperature over selected Mediterranean areas. Hydrol Earth Syst Sci 17(12):5041–5059

Dubrovsky M, Hayes M, Duce P, Trnka M, Svoboda M, Zara P (2014) Multi-GCM projections of future drought and climate variability indicators for the Mediterranean region. Reg Environ Change 14(5):1907–1919

European Environment Agency (2009) Water resources across Europe-confronting water scarcity and drought. EEA Report No 2/2009. http://www.eea.europa.eu/publications/water-resources-across-europe. Accessed 15 Dec 2015

Fiseha BM, Setegn SG, Melesse AM, Volpi E, Fiori A (2014) Impact of climate change on the hydrology of upper Tiber River Basin using bias corrected regional climate model. Water Resour Manag 28(5):1327–1343

García-Ruiz JM, López-Moreno JI, Vicente-Serrano SM, Lasanta–Martínez S. T, Begueía S (2011) Mediterranean water resources in a global change scenario. Earth Sci Rev 105(3):121–139

Giorgi F (2006) Climate change hot-spots. Geophys Res Lett 33:L08707

Giorgi F, Lionello P (2008) Climate change projections for the Mediterranean region. Global Planet Change 63(2):90–104

Graham LP, Andréasson J, Carlsson B (2007) Assessing climate change impacts on hydrology from an ensemble of regional climate models, model scales and linking methods—a case study on the Lule River basin. Clim Change 81(S1):293–307

Hellenic Ministry for the Environment, Energy and Climate Change-Special Secretariat for Water (2014) Compilation of management plan for the river basins of Thessaly water district (GR08)-management plan. Special Secretariat for Water, Athens

Herrmann F, Keller L, Kunkel R, Vereecken H, Wendland F (2015) Determination of spatially differentiated water balance components including groundwater recharge on the Federal State level—a case study using the mGROWA model in North Rhine-Westphalia (Germany). J Hydrol Reg Stud 4:294–312

Jacob D (2001) A note to the simulation of the annual and inter-annual variability of the water budget over the Baltic Sea drainage basin. Meteorol Atmos Phys 77(1–4):61–73

Jacob D, Bärring L, Christensen OB, Christensen JH, de Castro M, Déqué M, Giorgi F, Hagemann S, Hirschi M, Jones R, Kjellström E, Lenderink G, Rockel B, Sánchez E, Schär C, Seneviratne SI, Somot S, van Ulden A, van den Hurk B (2007) An inter-comparison of regional climate models for Europe: model performance in present-day climate. Clim Change 81:31–52

Jacobeit J, Hertig E, Seubert S, Lutz K (2014) Statistical downscaling for climate change projections in the Mediterranean region: methods and results. Reg Environ Change 14(5):1891–1906

Kalogeropoulos K, Chalkias C (2013) Modelling the impacts of climate change on surface runoff in small Mediterranean catchments: empirical evidence from Greece. Water Environ J 27(4):505–513

Kjellström E, Bärring L, Gollvik S, Hansson U, Jones C, Samuelsson P, Rummukainen M, Ullerstig A, Willén U and Wyser K (2005) A 140-year simulation of European climate with the new version of the Rossby Centre regional atmospheric climate model (RCA3). Reports Meteorology and Climatology, 108, SMHI, SE-60176 Norrköping, Sweden, p. 54

Koutroulis AG, Grillakis MG, Daliakopoulos IN, Tsanis IK, Jacob D (2016) Cross sectoral impacts on water availability at + 2 °C and + 3 °C for east Mediterranean island states: the case of Crete. J Hydrol 532:16–28

Koutsoyiannis D and Mimikou M (1996) Country Paper for Greece, Management and Prevention of Crisis Situations: Floods, Droughts and Institutional Aspects. 3rd EURAQUA Technical Review, Rome, 63–77, EURAQUA. https://www.itia.ntua.gr/getfile/69/1/documents/1996EuraquaFloods.pdf. Accessed 15 Dec 2015

Loukas A (2010) Surface water quantity and quality assessment in Pinios River, Thessaly, Greece. Desalination 250(1):266–273

Loukas A, Vasiliades L (2004) Probabilistic analysis of drought spatiotemporal characteristics in Thessaly region, Greece. Nat Hazards Earth Syst Sci 4(5/6):719–731

Loukas A, Mylopoulos N, Vasiliades L (2007) A modeling system for the evaluation of water resources management strategies in Thessaly, Greece. Water Resour Manag 21(10):1673–1702

Ludwig R, Roson R, Zografos C, Kallis G (2011) Towards an interdisciplinary research agenda on climate change, water and security in Southern Europe and neighboring countries. Environ Sci Policy 14(7):794–803

Milano M, Ruelland D, Fernandez S, Dezetter A, Fabre J, Servat E, Fritsch J-M, Ardoin-Bardin S, Thivet G (2013) Current state of Mediterranean water resources and future trends under climatic and anthropogenic changes. Hydrol Sci J 58(3):498–518

Mimikou MA, Baltas EA (2013) Assessment of climate change impacts in Greece: a general overview. Am J Clim Change 3:46–56

Mimikou MA, Baltas E, Varanou E, Pantazis K (2000) Regional impacts of climate change on water resources quantity and quality indicators. J Hydrol 234(1):95–109

Navarra A, Tubiana L (2013) Regional assessment of climate change in the Mediterranean. Springer, Dordrecht

Panagopoulos A, Kassapi KA, Arampatzis G, Perleros B, Drakopoulou S, Tziritis E, Chrysafi A and Vrouhakis I (2012) Assessment of chemical and quantitative status of groundwater systems in Pinios hydrological basin- Greece. In: Proceeding of XI International Conference of Protection and Restoration of the Environment, Thessaloniki, pp 511–517

Panagopoulos A, Arampatzis G, Tziritis E, Pisinaras V, Herrmann F, Kunkel R, Wndland F (2016) Assessment of climate change impact in the hydrological regime of River Pinios Basin, central Greece. Desalination Water Treat 57:2256–2267

Pisinaras V (2016) Assessment of future climate change impacts in a Mediterranean aquifer. Global NEST J 18(1):119–130

Pisinaras V, Wei Y, Barring L, Gemitzi A (2014) Conceptualizing and assessing the effects of installation and operation of photovoltaic power plants on major hydrologic budget constituents. Sci Total Environ 493:239–250

Schröter D, Cramer W, Leemans R, Prentice IC, Araújo MB, Arnell NW, Bondeau A, Bugmann H, Carter TR, Garcia CA, de la Vega-Leinert AC, Erhard M, Ewert F, Glendining M, House JI, Kankaanpää S, Klein RJT, Lavorel S, Lindner M, Metzger MJ, Meyer J, Mitchell TD, Reginster I, Rounsevell M, Sabaté S, Sitch S, Smith B, Smith J, Smith P, Sykes MT, Thonicke K, Thuiller W, Tuck G, Zaehle S, Zierl B (2005) Ecosystem service supply and vulnerability to global change in Europe. Science 310(5752):1333–1337

Taylor KE (2001) Summarizing multiple aspects of model performance in a single diagram. J Geophys Res Atmos 106(D7):7183–7192

Teutschbein C, Seibert J (2013) Is bias correction of Regional Climate Model (RCM) simulations possible for non-stationary conditions? Hydrol Earth Syst Sci 17:5061–5077

Tolika K, Anagnostopoulou C, Maheras P, Vafiadis M (2008) Simulation of future changes in extreme rainfall and temperature conditions over the Greek area: a comparison of two statistical downscaling approaches. Global Planet Change 63:132–151

Tolika CK, Zanis P, Anagnostopoulou C (2012) Regional climate change scenarios for Greece: future temperature and precipitation projections from ensembles of RCMs. Global Nest Journal 14(4):407–421

van der Linden P, Mitchell JFB (2009) ENSEMBLES: Climate Change and its Impacts: Summary of research and results from the ENSEMBLES project. Met Office Hadley Centre, UK

van Meijgaard E, van Ulft LH, van de Berg WJ, Bosveld FC, van den Hurk BJJM, Lenderink G and Siebesma AP (2008) The KNMI regional atmospheric climate model RACMO version 2.1, KNMI Technical Report 302, p. 43. http://www.knmi.nl/bibliotheek/knmipubTR/TR302.pdf. Accessed 15 Dec 2015

Varanou E, Gkouvatsou E, Baltas E, Mimikou M (2002) Quantity and quality integrated catchment modeling under climate change with use of soil and water assessment tool model. J Hydrol Eng 7(3):228–244

Vasiliades L, Loukas A, Patsonas G (2009) Evaluation of a statistical downscaling procedure for the estimation of climate change impacts on droughts. Nat Hazards Earth Syst Sci 9(3):879

Zanis P, Kapsomenakis I, Philandras C, Douvis K, Nikolakis D, Kanellopoulou E, Zerefos C, Repapis C (2009) Analysis of an ensemble of present day and future regional climate simulations for Greece. Int J Climatol 29:1614–1633